Published in final edited form as:
Prostate. 2007 September 15; 67(13): 1447–1455. doi:10.1002/pros.20632.

High Resolution Oligonucleotide CGH Using DNA From Archived Prostate Tissue

Pamela L. Paris[1], **Shivaranjani Sridharan**[1], **Alicia Scheffer**[2], **Anya Tsalenko**[2], **Laurakay Bruhn**[2], and **Colin Collins**[1,*]

[1] Department of Urology, Comprehensive Cancer Center, University of California at San Francisco, San Francisco, California

[2] Life Sciences and Nanotechnology Department, Agilent Laboratories, Santa Clara, California

Abstract

BACKGROUND—The current focus on biomarker discovery is a result of an improved understanding of the biological basis for carcinogenesis and advances in technology. Biomarkers can aid in diagnosis, prognosis, treatment selection, and drug development. There is an urgent need for high-resolution tools that perform well using archived tissue for biomarker discovery and tools that can translate into the clinic.

METHODS—Oligonucleotide array comparative genomic hybridization (oCGH) was compared to BAC-based aCGH using unamplified total genomic DNA from formalin fixed paraffin-embedded (FFPE) prostate tissue.

RESULTS—The copy number aberrations detected with the BAC and oligonucleotide arrays were highly correlated in cases where the arrays contained probes in similar genomic locations. The oligonucleotide array platform provided more precise mapping due to the higher density of oligonucleotide probes.

CONCLUSIONS—These results demonstrate the utility of high-resolution oligonucleotide arrays designed to use genomic DNA for CGH measurements using archived tissue samples for discovery and clinic based assays.

Keywords

FFPE; aCGH; oCGH; biopsy

INTRODUCTION

Array comparative genomic hybridization (aCGH) is a valuable tool for identifying DNA copy number changes in tumor genomes. Genomic copy number alterations can lead to altered expression of oncogenes and tumor suppressor genes. Moreover, copy number abnormalities can be associated with the clinical course of the disease and used for selection of therapy. Detailed mapping of amplicons and deletions localizes potential therapeutic targets. Formalin-fixed paraffin-embedded (FFPE) tumor specimens provide a rich source of patient samples for these studies, and often with corresponding long follow-up data. FFPE samples yield DNA that is often degraded and therefore more challenging to use for aCGH. Our published DNA extraction methods, utilized in this manuscript, allows for routine processing of FFPE tissue from a variety of sources [1]. The use of FFPE prostate tissue on BAC-based arrays has been

*Correspondence to: Colin Collins, UCSF Box 0808, San Francisco, CA 94143. collins@cc.ucsf.edu.

demonstrated previously by our laboratory [1]. Recently, oligonucleotide array based CGH platforms have emerged with the potential for more flexible array design and higher-resolution copy number mapping [2–4] thus, significantly increasing the power of studies aimed at discovery of new therapeutic and diagnostic targets. Combined with biomarkers of aggressive disease, such technologies could translate directly into the clinic. This is of particular relevance to prostate cancer where over detection and over treatment are significant despite a protracted and non-life threatening natural history in many men [5]. Therefore, it is important to couple biomarkers and technologies that will work well with FFPE biopsy specimens. We report on the use of genomic DNA from FFPE prostate tumors using the Agilent oligonucleotide CGH (oCGH) platform and the comparison of these results to those obtained using UCSF scanning BAC arrays. Application of Agilent arrays for analysis of FFPE biopsy specimens is also demonstrated.

MATERIALS AND METHODS

DNA from four different radical prostatectomy cases (designated 13P, 33P, 34P, and 41P) was isolated from FFPE tissue. A single pathologist outlined areas of greater than 75% tumor for macrodissection with a scalpel. DNA was extracted from the tissue scrapings using the Puregene DNA isolation kit (Gentra) as per the manufacturer's instructions. Two phenol:-chloroform extractions followed by an ethanol precipitation were performed after the Gentra kit's final elution step. The biopsy specimen from a routine fine needle, biopsy was embedded in an FFPE block. An H&E guide slide was used to macrodissect tumor tissue (>90%) from 10 slides of 10 μm thickness. The tissue was digested using proteinase K for 48 hr at 56μC. Genomic DNA was isolated using the Qiagen (Valencia, CA) QIAamp DNA Micropurification kit using the manufacturer's protocol for biopsy specimens. This was followed by an ethanol precipitation. DNA was quantitated using the Nanodrop spectrophotometer. DNA quality was assessed by the 260:280 ratio and its integrity by agarose gel ethidium bromide visualization. The DNAs were found to be of typical quality in terms of purity and the amount of degradation observable by gel electrophoresis.

aCGH was performed using BAC arrays containing 2,460 BAC clones printed at UCSF as well as Agilent Human Genome 44 or 244 K 60 mer oligonucleotide arrays containing approximately 40,000 probes with an average spatial resolution of ~35 kb or 244,000 probes with an average resolution of ~9 kb. The BAC aCGH was performed as described in Paris et al. [1] with a male reference DNA (Promega). The standard oligonucleotide oCGH experiments were performed as per the manufacturer's instructions (http://chem.agilent.com/scripts/LiteraturePDF.asp?iWHID=39980) with the following exceptions: the input DNA was lessened from 2 to ~1 μg, the hybridization time was increased from 40 to 65 hr and wash 3 was not performed. Prostate samples 13P and 33P were hybridized with female reference DNA (Promega) in dye flip pairs to provide an additional source of confidence in copy number calls. Additional oligonucleotide array experiments were performed for sample 13P, 34P, and 41P and the biopsy using only 500 ng DNA to ascertain the utility of working with low genomic yield samples. Components of labeling and hybridization were identical to standard reactions, except the DNA was digested with restriction enzymes Alu1 and Rsa1 for only 2 hr followed immediately (without cleanup) by fluorescent labeling for 1 hr, and hybridization was carried out for 40 hr. The 500 ng prostate sample was hybridized with male reference DNA. Agilent Feature Extraction software version 8.1.1.1 was used to extract feature level data from the Agilent Microarray Scanner files.

Regions of copy number gain and loss for the BAC aCGH data were identified by creating sample specific thresholds [6,7]. The clones with $\log_2$ ratios above or below +/− a tumor sample's threshold value were considered as gains or losses, respectively. The aberration detection module-1 (ADM-1) aberration detection algorithm from Agilent's CGH Analytics

software was used to identify regions of copy number gain or loss from both the oligonucleotide and BAC CGH data [8]. Briefly, ADM-1 identifies aberrant genomic intervals based on a statistical score. This score is calculated as the average $\log_2$ ratio of probes in the interval, multiplied by the square root of the number of such probes and divided by the derivative $\log_2$ ratio spread of the array. Aberration calls were made for each experiment after initial preprocessing of the data that included combining $\log_2$ ratios for replicate probes and centralization. In the centralization step, all $\log_2$ ratios are shifted by an array-specific constant, such that ADM-1 applied to shifted $\log_2$ ratios calls the minimum number of probes aberrant. The centralization step was applied only to the oligonucleotide data.

RESULTS AND DISCUSSION

aCGH and oCGH were performed with DNA isolated from FFPE preserved samples from four different radical prostatectomy cases (designated 13P, 33P, 34P, 41P) using both BAC arrays containing 2,460 BAC clones printed at UCSF as well as Agilent's Human Genome 44 or 244 K 60 mer oligonucleotide arrays containing approximately 40,000 and 244,000 probes, respectively. Samples were selected to represent both good (≥12 kb) and poor quality (≥500 bp) DNA that is obtained from FFPE tissue. All samples were archived for 8 years prior to processing, except sample 41P which was 6 years old.

Detailed comparison of aberration calls made from the 44 K oligonucleotide and BAC array data was performed for FFPE samples 13P and 33P, with the focus being regions where both platforms had overlapping probes. Dye flip experiments for the oligonucleotide data were combined, and aberrations were called using CGH Analytics aberration detection algorithm ADM-1 with a threshold of 6. Aberrations in BAC data were identified using the standard sample specific threshold method [6,7] and also using ADM-1. Aberrant intervals identified in the BAC data showed good agreement with corresponding intervals from the oligonucleotide data (Fig. 1 and Table I). We also computed the fraction of BAC probes above or below the sample specific threshold showing gain or loss that were inside oligonucleotide amplified or deleted intervals. For samples 13P and 33P, 82 and 90%, respectively, of BAC probes showing gain or loss were identified within oligonucleotide aberrant intervals.

There was good concordance observed between the overall copy number profiles across the genome obtained from the BAC and oligonucleotide array platforms for both samples 13P and 33P both in terms of the genomic position of the gains and losses and in the magnitude of the copy number differences (Fig. 1). The Pearson correlation of the average $\log_2$ ratios in matching aberrant regions was 0.87 and 0.96 for samples 13P and 33P, respectively. For example, deletion of the entire p arm on chromosome 8 for sample 13P was identified by an average $\log_2$ ratio in both the BAC and oligonucleotide data as 0.56. This deletion call was based on 59 BAC probes and 556 oligonucleotide probes, extending from 0 to 38 Mb in the BAC data and 0 to 43 Mb in the oligonucleotide data. A detailed visualization of the aberrations observed on chromosome 8 is highlighted in Figure 2A. Chromosome 8 was chosen because 8p is known to be commonly deleted in prostate cancer [9–11].

In some cases, the oligonucleotide array platform provided more precise mapping of aberration boundaries due to the higher density of oligonucleotide probes. The higher density of oligonucleotide probes can also add statistical confidence to copy number calls, especially where only one BAC probe maps to an aberration. An example highlighting this was found in sample 13P on chromosome 12 (p 12.1) where the same copy number change was observed in both the BAC and oligonucleotide array data. However, the aberration breakpoints were more precisely mapped in the oligonucleotide data due to the higher density of probes (Fig. 2B), thereby narrowing the number of candidate genes.

Oligonucleotide arrays developed specifically for CGH [2–4] and whole genome BAC tiling arrays [12] have the potential to provide very high-resolution copy number measurements. The goal of these experiments was to assess the quality of CGH data obtained with whole genome oligonucleotide arrays using clinically relevant, but challenging DNA from archived prostate tissue, that has been shown previously to work well using BAC arrays. The results from the oligonucleotide array platform correlated very well with the BAC array results although there were some instances of aberrations detected more robustly and with more precise mapping with the oligonucleotide arrays due to the higher probe density on these arrays. The only considerable differences were attributable to regions where clones were absent in the BAC data. It is note worthy that Agilent has selected probes biased toward genes, in particular cancer related genes (represented by a minimum of two probes), ensuring adequate coverage in the most commonly studied genomic regions.

In our hands, DNA extracted from frozen or FFPE tissue using our published protocols are equivalent for BAC-based aCGH and this is true regardless of the laboratory of source's fixation protocol [1,7,13]. This is consistent with a study published by Little et al. comparing frozen and FFPE DNA for CGH on BAC arrays. In the present study matched fresh frozen and fixed specimens could not be directly compared. To overcome this limitation, we embedded DUI45 prostate cancer cells to mimic routine frozen and FFPE archiving and compared extracted DNA on 244 K oCGH arrays to DNA extracted from unfixed DU145 cells on BAC arrays. The frozen and FFPE DNA produced concordant copy number profiles on the Agilent arrays and produced copy number profiles essentially identical to each other (Fig. 3). In addition, these profiles match our unpublished and others published BAC aCGH data for DU145 [14,15]. We chose to focus on FFPE material in this manuscript because it is commonly believed to be more difficult to work with than frozen material and because of its importance for translational research.

DNA yields from FFPE specimens may be small because many of the most informative experiments and clinical applications will need to begin with needle biopsies where yields may be in the range of 500 ng. Thus, it is significant that we obtained comparable oCGH results using only 500 ng of FFPE (Fig. 4). Figure 4A shows an overlay of BAC-based aCGH and oCGH using 1 μg DNA and oCGH using 500 ng DNA from sample 13P (Fig. 4A). Qualitative assessment of two additional oCGH 500 ng samples in Figure 4 shows great similarity with the corresponding aCGH data using 1 μg of DNA. The average $\log_2$ ratio standard deviation of the replicate probes randomly dispersed on the array, which serve as a measure of the quality of the array result, was 0.028 (34P) and 0.071 (41P). Next we extracted DNA from an FFPE prostate tumor biopsy and for analysis on the 244K oCGH platform. The average standard deviation of the $\log_2$ ratios for the replicate probes on the biopsy array was 0.039. A penetrance plot is shown for the copy number changes detected by oCGH for the biopsy and its matched primary tumor (Fig. 5). It may of interest to note the similarity between the two copy number plots despite the fact that distinct foci of the same tumor were analyzed.

CONCLUSIONS

To the best of our knowledge, this is the first report on the use of commercial oligonucleotide arrays with unamplified FFPE prostate biopsy and radical prostatectomy tissue. Van den Ijssel et al. [16] recently published a paper reporting the use of their in-house spotted oligonucleotide arrays with DNA from a single FFPE, gastric tumor. These authors report qualitatively similar results with their oligonucleotide platform and BAC arrays. In our report, we have conducted qualitative and quantitative comparisons and have used a commercially available oligonucleotide platform. This latter point is particularly relevant for future clinical applications since the FDA just recently approved an assay system that included the Agilent microarray (Agendia MammaPrint).

The use of archival tissue is very important for prostate cancer research due to its long protracted natural history. The value of PSA screening has long been a matter of debate. A recent study found that men who have been screened for prostate cancer by the most commonly used tests (PSA and DRE) have no greater chance of surviving the disease than those who have not been screened at all [17]. This highlights the need for the identification of new prognostic and predictive biomarkers that will compliment, and therefore improve upon existing clinical standards to help physicians and their patients make decisions regarding treatment. To the best of our knowledge this is the first time oCGH copy number data has been obtained using unamplified DNA from a FFPE tumor biopsy and its matched primary tumor. This should encourage utilization of biopsy specimens for basic and translational studies. oCGH's higher resolution will allow for better characterization of tumor genomes and therefore expedite the identification of genes driving progression and candidate therapeutic targets. The DNA extraction protocol followed in this paper is an essential step to obtaining DNA from FFPE tissue that is useable for aCGH and oCGH. Although we cannot generalize to all cancer tissue types, this DNA protocol has allowed us to obtain copy number profiles from DNA extracted from FFPE tissue obtained from multiple institutions around the world, regardless of the age of the sample (up to 16 years old). (1, 7, and unpublished data). Based on our experience, the UV–Vis values (260/280 ~1.8, 260/230 ~2) and DNA integrity (>500 bp) visualized by gel chromatography can determine whether a sample will perform well on a CGH array. A sample seems to fail due to the case, rather than the archival method (e.g., frozen vs. FFPE). The Agilent oligonucleotide platform and methods used in these studies provide high quality, reproducible oCGH copy number profiles from small amounts of FFPE extracted DNA and therefore, represents a valuable tool for biomarker discovery and possibly development of clinical assays.

Acknowledgments

Grant sponsor: UCSF Prostate Cancer SPORE, NIH; Grant number: P50CA89520.

This work was supported by the UCSF Prostate Cancer SPORE, NIH Grant P50CA89520. We would like to thank Dr. Peter Carroll, Dr. Jeffry Simko, and Dr. Giancarlo Albo for assistance with sample acquisition, pathology and DNA extraction, respectively. We are very appreciative of the programming assistance from Emmanuel Yera. In addition, the authors also thank Amir Ben-Dor and Zohar Yakhini from Agilent Laboratories for helpful discussions on data analysis.

References

1. Paris PL, Albertson DG, Alers JC, Andaya A, Carroll P, Fridlyand J, Jain AN, Kamkar S, Kowbel D, Krijtenburg PJ, Pinkel D, Schroder FH, Vissers KJ, Watson VJ, Wildhagen MF, Collins C, Van Dekken H. High-resolution analysis of paraffin-embedded and formalin-fixed prostate tumors using comparative genomic hybridization to genomic microarrays. Am J Pathol 2003;162(3):763–770. [PubMed: 12598311]
2. Brennan C, Zhang Y, Leo C, Feng B, Cauwels C, Aguirre AJ, Kim M, Protopopov A, Chin L. High-resolution global profiling of genomic alterations with long oligonucleotide microarray. Cancer Res 2004;64(14):4744–4748. [PubMed: 15256441]
3. Carvalho B, Ouwerkerk E, Meijer GA, Ylstra B. High resolution microarray comparative genomic hybridisation analysis using spotted oligonucleotides. J Clin Pathol 2004;57(6):644–646. [PubMed: 15166273]
4. Barrett MT, Scheffer A, Ben-Dor A, Sampas N, Lipson D, Kincaid R, Tsang P, Curry B, Baird K, Meltzer PS, Yakhini Z, Bruhn L, Laderman S. Comparative genomic hybridization using oligonucleotide microarrays and total genomic DNA. Proc Natl Acad Sci USA 2004;101(51):17765–17770. [PubMed: 15591353]
5. Cooperberg MR, Moul JW, Carroll PR. The changing face of prostate cancer. J Clin Oncol 2005;23(32):8146–8151. [PubMed: 16278465]

6. Fridlyand J, Snijders AM, Pinkel D, Albertson DG, Jain A. Application of Hidden Markov Models to the analysis of the array CGH data. J Multivar Anal (Special Genomic Issue) 2004;90:132–153.
7. Paris PL, Andaya A, Fridlyand J, Jain AN, Weinberg V, Kowbel D, Brebner JH, Simko J, Watson JE, Volik S, Albertson DG, Pinkel D, Alers JC, van der Kwast TH, Vissers KJ, Schroder FH, Wildhagen MF, Febbo PG, Chinnaiyan AM, Pienta KJ, Carroll PR, Rubin MA, Collins C, van Dekken H. Whole genome scanning identifies genotypes associated with recurrence and metastasis in prostate tumors. Hum Mol Genet 2004;13(13):1303–1313. [PubMed: 15138198]
8. Lipson, D.; Aumann, Y.; Ben-Dor, A.; Linial, N.; Yakhini, Z. Proceedings of RECOMB ’05, LNCS 3500; Springer-Verlag; 2005. p. 83
9. Cher ML, MacGrogan D, Bookstein R, Brown JA, Jenkins RB, Jensen RH. Comparative genomic hybridisation, allelic imbalance, and fluorescence in situ hybridization on chromosome 8 in prostate cancer. Genes Chromosomes Cancer 1994;11(3):153–162. [PubMed: 7530484]
10. Matsuyama H, Pan Y, Yoshihiro S, Kudren D, Naito K, Bergerheim US, Ekman P. Clinical significance of chromosome 8p, 10q, and 16q deletions in prostate cancer. Prostate 2003;54(2):103–111. [PubMed: 12497583]
11. Oba K, Matsuyama H, Yoshihiro S, Kishi F, Takahashi M, Tsukamoto M, Kinjo M, Sagiyama K, Naito K. Two putative tumor suppressor genes on chromosome arm 8p may play different roles in prostate cancer. Cancer Genet Cytogenet 2001;124(1):20–26. [PubMed: 11165318]
12. Ishkanian AS, Malloff CA, Watson SK, DeLeeuw RJ, Chi B, Coe BP, Snijders A, Albertson DG, Pinkel D, Marra MA, Ling V, MacAulay C, Lam WL. A tiling resolution DNA microarray with complete coverage of the human genome. Nat Genet 2004;36(3):299–303. [PubMed: 14981516]
13. Paris PL, Hofer MD, Albo G, Kuefer R, Gschwend JE, Hautmann RE, Fridyland J, Simko J, Carroll PR, Rubin MA, Collins C. Genomic profiling of hormone-naive lymph node metastases in patients with prostate cancer. Neoplasia 2006;8(12):1083–1089. [PubMed: 17217626]
14. Bernardino J, Bourgeois CA, Muleris M, Dutrillaux AM, Malfoy B, Dutrillaux B. Characterization of chromosome changes in two human prostatic carcinoma cell lines (PC-3 and DU145) using chromosome painting and comparative genomic hybridization. Cancer Genet Cytogenet 1997;96(2):123–128. [PubMed: 9216719]
15. Nupponen NN, Hyytinen ER, Kallioniemi AH, Visakorpi T. Genetic alterations in prostate cancer cell lines detected by comparative genomic hybridization. Cancer Genet Cytogenet 1998;101(1):53–57. [PubMed: 9460501]
16. van den Ijssel P, Tijssen M, Chin SF, Eijk P, Carvalho B, Hopmans E, Holstege H, Bangarusamy DK, Jonkers J, Meijer GA, Caldas C, Ylstra B. Human and mouse oligonucleotide-based array CGH. Nucleic Acids Res 2005;33(22):e192. [PubMed: 16361265]
17. Concato J, Wells CK, Horwitz RI, Penson D, Fincke G, Berlowitz DR, Froehlich G, Blake D, Vickers MA, Gehr GA, Raheb NH, Sullivan G, Peduzzi P. The effectiveness of screening for prostate cancer: A nested case-control study. Arch Intern Med 2006;166(1):38–43. [PubMed: 16401808]

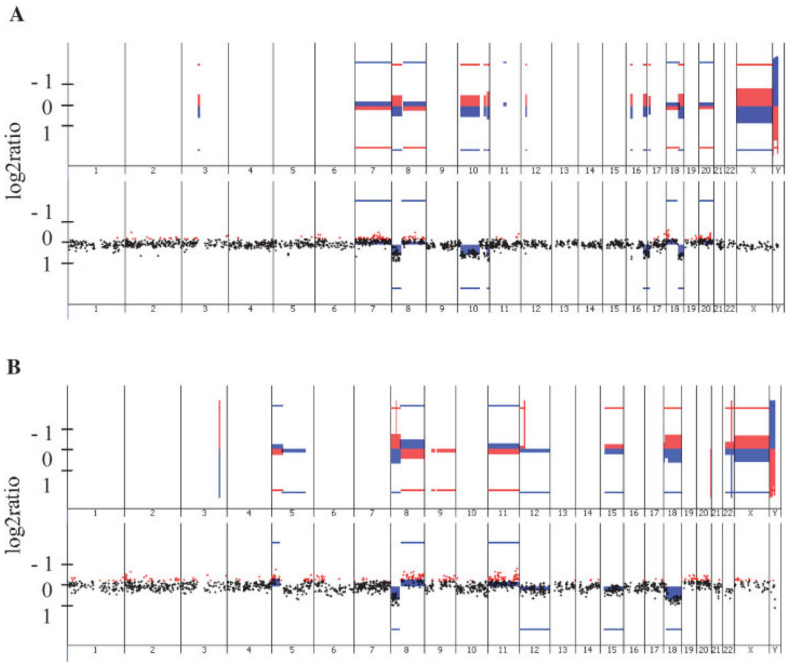

Fig. 1.

Genome view of a CGH aberration calls for samples 13P (**A**) and 33P (**B**). The **upper panel** of each set shows the oligonucleotide array dye flip pair results and the **lower panel** displays the BAC array results, both display $\log_2$ ratio splotted as a function of chromosomal position using Agilent's CGH Analytics software. For both the oligonucleotide and BAC data plots, aberration calls from ADM-1 (threshold 10) in positive polarity are shown with blue lines, aberration calls in negative polarity (i.e., dye flip) are shown with red lines. The heights of the corresponding shaded rectangles indicate average $\log_2$ ratio in each aberrant interval. To enable easier visualization of the aberrant intervals, $\log_2$ ratios from individual oligonucleotide probes are not shown. For the BAC aCGH plots, $\log_2$ ratios from individual probes are plotted as a function of chromosomal position with copy number gains in red ($\log_2$ ratio >0.25) and losses in green ($\log_2$ ratio <−0.25). Note the good concordance between the oligonucleotide and BAC aberration calls displayed as blue horizontal bars, as well as the consistency between the dye flip pairs displayed as red and blue horizontal bars from the oligonucleotide experiments.

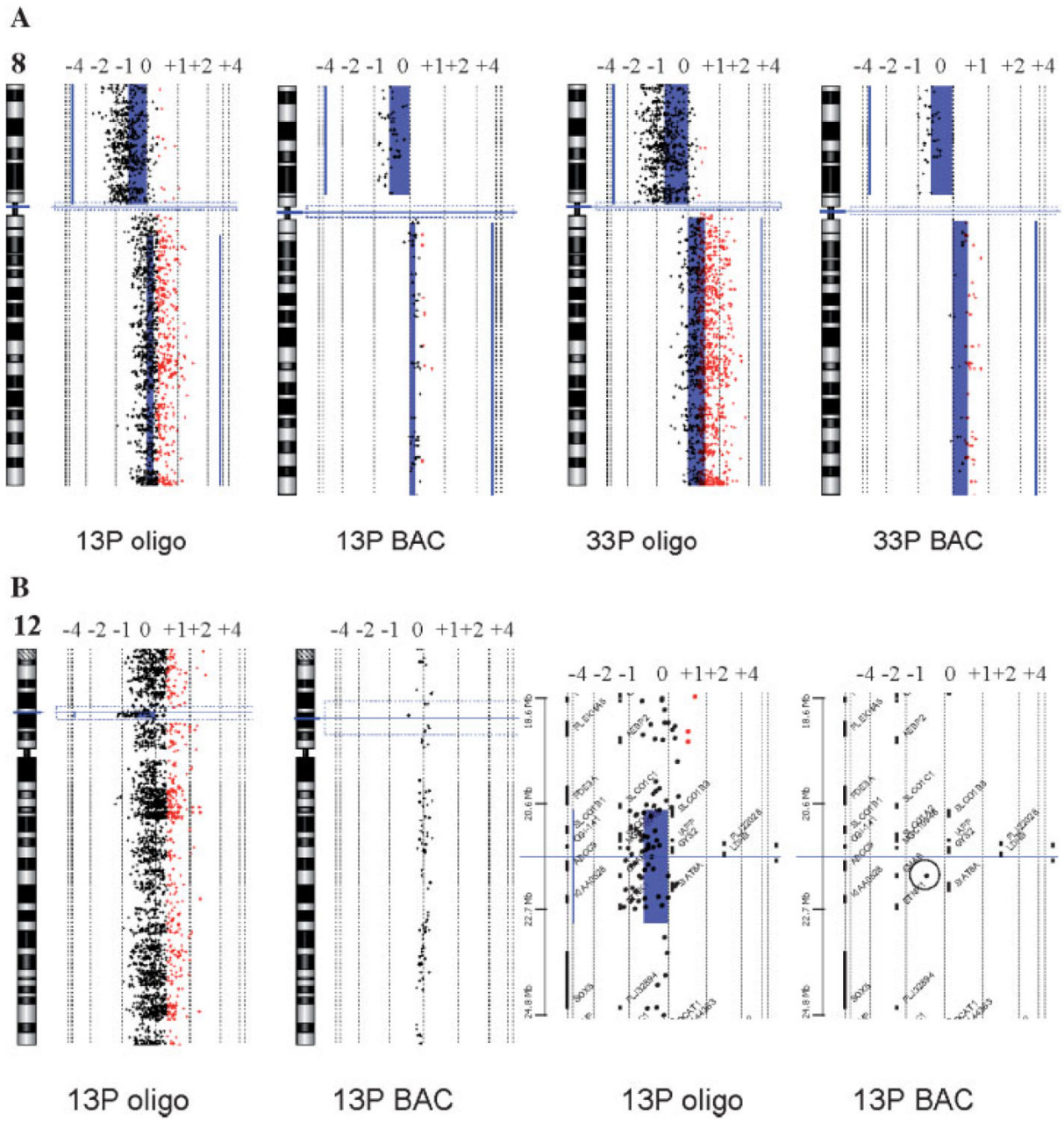

Fig. 2.

Detailed view of oligonucleotide and BAC aCGH data on chromosomes 8 and 12. Log_2 ratios are plotted for each probe as a function of chromosomal position. Probes with log_2 ratio >0.25 are shown in red, probes with log_2 ratio <−0.25 are shown in green. Vertical blue lines show the extent of the deleted intervals while the width of the blue rectangles correspond to theaveragelog_2 ratio of the probes inside a given aberration interval. (**A**) Sample 13P and 33P oligonucleotide and BAC array data plots. Whole arm loss of 8p and gain of 8q were detected with both techniques for both samples. (**B**) Sample 13P oligonucleotide and BAC array data is plotted in the first two panels, respectively, showing all of chromosome 12. The right two panels show a zoomed-in subregion of chromosome 12 near p 12.3. Gray bars indicate specific genes in this region. A single BAC probe with a log_2 ratio consistent with a loss (circled) agrees

with the aberration call in the oligonucleotide data, however the increased density of probes on the oligonucleotide array in this region enables are fined view of the breakpoints flanking the deleted region.

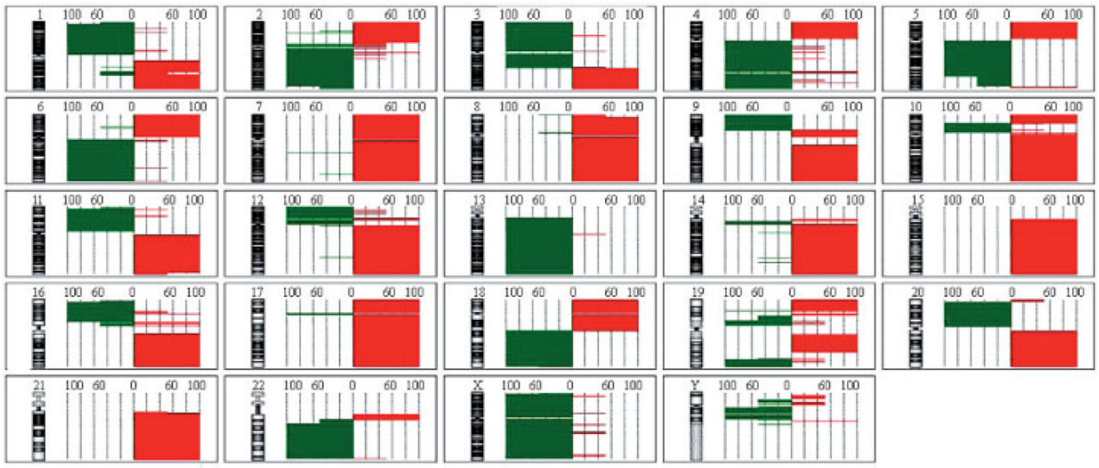

Fig. 3.

DU145 fresh and fixed tissue penetrance plot for the frozen and FFPE 244KoCGH data. The frequency of a copy number call at a particular locus is shown for each chromosome, with gains in red and losses in green.

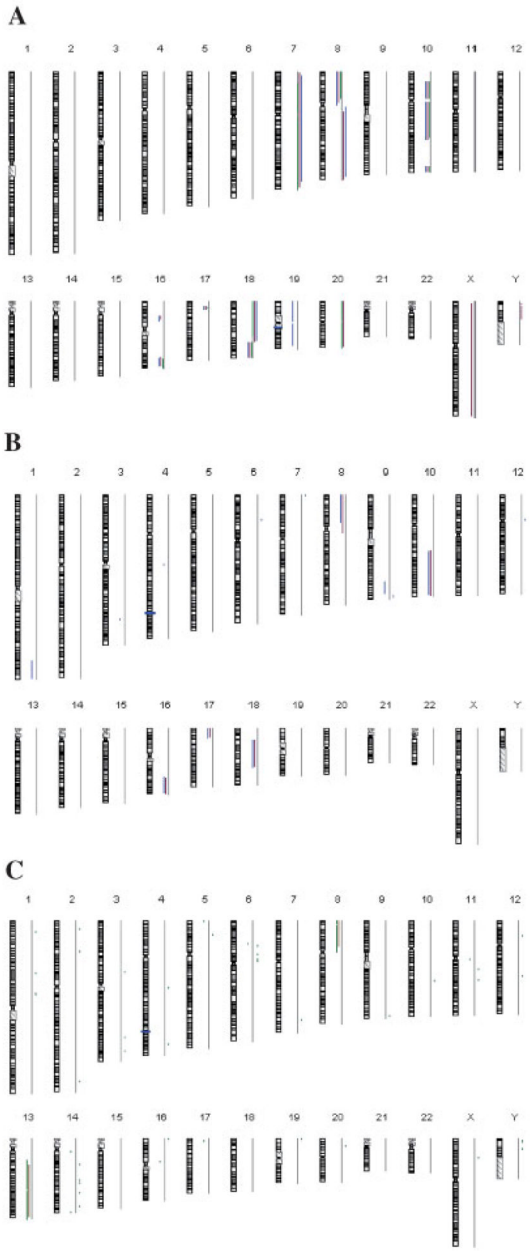

Fig. 4.

Genome view of aCGH and oCGH aberration calls using Agilent's CGH Analytics software. **A**: Sample 13P 44KoCGH with 1 μg sample input (purple) and oCGH with 500 ng input (blue), and BAC aCGH with 1 μg input (green). Aberration calls from ADM-1 are shown with vertical lines, in each sample's respective color, next to the ideograms. Gains are depicted with vertical lines to the right and losses to the left of the gray vertical line corresponding to each chromosome. **B**,**C**: Additional FFPE samples on oCGH with 500 ng input DNA.41P 44KoCGHinblue and BAC aCGH in purple (**panel B**) and similarly 34P 244KoCGHin green and BAC aCGH in brown (**panel C**).

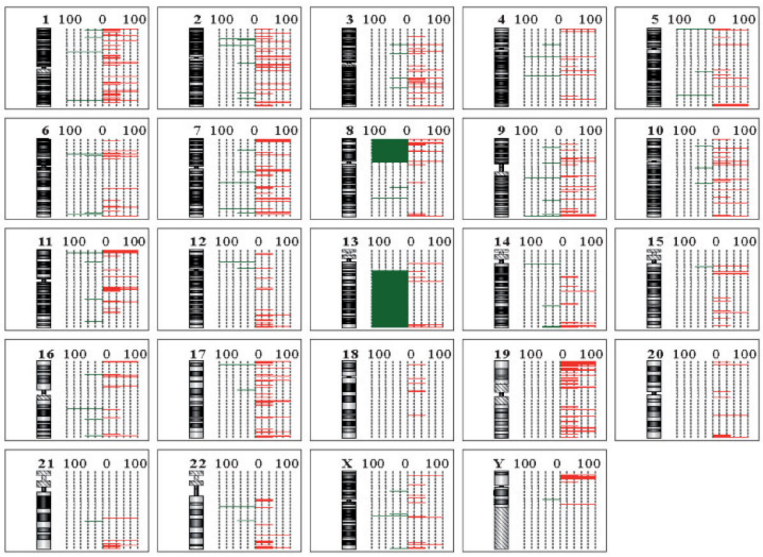

Fig. 5.

FFPE prostate biopsy and matched primary oCGH penetrance plot. Both samples were run with 500 ng unamplified DNA on Agilent's 244K oCGH platform. The frequency of gains and deletions are shown in red and green, respectively, for each chromosome.

TABLE I

Comparison of Aberration Calls Made by ADM-1 Algorithm for BAC and Oligonucleotide Data

(a) Sample 13P

BAC data							Oligo data					
Chromosome	BAC interval start Mb	BAC interval end Mb	BAC ADM-1 score	Average $\log_2$ ratio in BAC data	Number of BAC probes in the interval	BAC probes with $\lvert\log_2$ ratio$\rvert$ >0.3	Oligo interval start Mb	Oligo interval end Mb	Oligo ADM-1 score	Average $\log_2$ ratio in oligo interval	Number of oligo probes in the interval	Overlap of BAC and oligo intervals
5	67.25437	67.8193	−7.8	−0.53	3	3	66.23876	68.53649	−8	−0.59	20	Yes
7	0.188013	158.5457	19.4	0.17	185	28	1.944812	156.4748	29.5	0.22	1,998	Yes
7	79.45866	119.3219	5.3	0.26	51	18	1.944812	156.4748	29.5	0.22	1,998	Yes
8	0.000001	38.25725	−32.9	−0.56	59	44	0.18136	43.07369	−39.9	−0.56	556	Yes
8	47.82246	146.309	12.7	0.18	84	13	52.8601	146.1261	24.7	0.25	1,068	Yes
10	14.45467	89.67623	−35.8	−0.55	62	57	14.05411	91.60646	−50.6	−0.57	874	Yes
10	114.1858	115.8874	−9.3	−0.54	4	4	113.3667	116.4514	−11.4	−0.55	48	Yes
10	128.2415	135.0374	−16.1	−0.62	9	8	127.9043	134.878	−20.8	−0.73	90	Yes
16	23.51751	23.8141	−8.7	−0.71	2	2	20.74787	24.75474	−19.0	−0.65	96	Yes
16	76.93748	90.04213	−17.2	−0.53	14	14	76.62921	89.85362	−32	−0.62	299	Yes
17	7.040603	10.06614	−13.6	−0.56	8	8	7.146866	11.92604	−19	−0.49	162	Yes
18	0.636259	46.73048	13.4	0.28	31	11	0.571121	54.11426	16	0.22	606	Yes
18	54.59628	76.11534	−20.3	−0.63	16	14	54.21252	76.08127	−32.1	−0.66	262	Yes
20	0.306441	63.74207	15.1	0.19	96	12	0.158467	63.5226	18.4	0.18	1,102	Yes
X	6.598801	148.1754	−6.7	−0.10	57	2	2.295272	153.2735	−117.1	−0.91	1,823	Yes

(b) Sample 33P

BAC data							Oligo data					
Chromosome	BAC interval start Mb	BAC interval end Mb	BAC ADM-1 score	Average $\log_2$ ratio in BAC data	Number of BAC probes in the interval	BAC probes with $\lvert\log_2$ ratio$\rvert$ >0.41	Oligo interval start Mb	Oligo interval end Mb	Oligo ADM-1 score	Average $\log_2$ ratio in oligo interval	Number of oligo probes in the interval	Overlap of BAC and oligo intervals
5	1.477795	33.74721	11.7	0.39	23	10	0.147811	45.87533	19.4	0.30	440	Yes

(b) Sample 33P

BAC data							Oligo data					
Chromosome	**BAC interval start Mb**	**BAC interval end Mb**	**BAC ADM-1 score**	**Average $\log_2$ ratio in BAC data**	**Number of BAC probes in the interval**	**BAC probes with $\lvert\log_2$ ratio$\rvert$ >0.41**	**Oligo interval start Mb**	**Oligo interval end Mb**	**Oligo ADM-1 score**	**Average $\log_2$ ratio in oligo interval**	**Number of oligo probes in the interval**	**Overlap of BAC and oligo intervals**
5	53.34516	133.5579	−9.0	−0.21	46	5	55.16637	141.5624	−17.8	−0.18	1,049	Yes
6	55.30227	170.7381	−8.5	−0.21	43	5	63.0039	170.749	−14.1	−0.13	1,271	Yes
8	0.000001	38.25725	−27.6	−0.67	59	38	0.18136	43.07369	−57.4	−0.79	556	Yes
8	49.11755	146.309	19.0	0.38	83	28	47.55326	146.285	53.4	0.52	1,107	Yes
9	84.01766	131.8795	9.2	0.22	55	4	31.18137	136.0045	22.2	0.20	1,307	Yes
10	2.196985	135.0374	−7.9	−0.11	126	5	1.000679	134.878	−21.6	−0.17	1,721	Yes
11	0.000001	133.5895	17.5	0.23	173	26	0.18679	133.984	43.5	0.29	2,296	Yes
12	0.000001	129.158	−12.1	−0.21	90	10	0.179153	132.0071	−27.7	−0.19	2,189	Yes
15	21.35961	100.2569	−11.7	−0.23	67	9	20.41443	100.0866	−30.9	−0.27	1,318	Yes
18	10.74993	76.11534	−25.9	−0.68	36	32	9.878349	76.08127	−64.2	−0.75	755	Yes
19	0.902441	62.47401	9	0.25	36	6	0.79864	63.78317	8.5	0.06	2,090	Yes
20	17.70828	53.18655	9	0.21	51	4	0.133969	63.5226	16.4	0.16	1,103	Yes
22	15.54704	43.99559	−6.8	−0.29	16	2	14.86926	49.17607	−30.1	−0.33	831	Yes
11	118.8619	133.5895	6.4	0.49	14	9						No
14	23.85832	54.17806	−7.1	−0.25	23	2	22.83116	101.4375	−6.3	−0.06	1,168	No
6	33.78701	44.16825	6.7	0.30	13	3	24.91239	32.04199	5.9	0.12	240	No

Table shows all aberrant intervals identified in the BAC data by ADM-1 algorithm with threshold of 6, together with corresponding oligonucleotide intervals. For each interval we report start position, end position, ADM-1 score, average $\log_2$ ratio, and the number of probes in the interval. In addition, we report the number of BAC probes in the interval exceeding the sample specific threshold used to call gains and losses in the BAC data (0.41 for sample 33P and 0.3 for sample 13P).